Printing Cu on Cold Sprayed Cu Plate via Selective Laser Melting– A Hybrid Additive Manufacturing

Qing Chai *, Chaoxin Jiang, Chunjie Huang, Yingchun Xie, Xingchen Yan, Rocco Lupoi, Chao Zhang, Shuo Yin *

Posted Date: 12 September 2023

doi: 10.20944/preprints202309.0776.v1

Keywords: Cold spraying; Selective laser melting; Microstructure characteristics; Hardness and interfacial bonding strength

Article

Printing Cu on Cold Sprayed Cu Plate via Selective Laser Melting–A Hybrid Additive Manufacturing

Qing Chai [1]*, Chaoxin Jiang [1], Chunjie Huang [2], Yingchun Xie [3], Xingchen Yan [3], Rocco Lupoi [4], Chao Zhang [1] and Shuo Yin [1,4,*]

[1] College of Mechanical Engineering, Yangzhou University, 225127 Yangzhou, China
[2] Materials Technology, Helmut-Schmidt-University/University of the Federal Armed Forces Hamburg, 22043 Hamburg, Germany
[3] The Key Lab of Guangdong for Modern Surface Engineering Technology, National Engineering Laboratory for Modern Materials Surface Engineering Technology, Institute of New Materials, Guangdong Academy of Sciences, Guangzhou 510651, China
[4] Trinity College Dublin, The University of Dublin, Department of Mechanical and Manufacturing Engineering, Parsons Building, Dublin 2, Ireland
* Correspondence: chaiqing@yzu.edu.cn

Abstract: The development of the additive manufacturing (AM) technology proffers challenging requirements for forming accuracy and efficiency. In this paper, a hybrid additive manufacturing technology combining fusion-based selective laser melting (SLM) and solid-state cold spraying (CS) was proposed in order to enable the fast production of near-net-shape metal parts. The idea is to fabricate a bulk deposit with a rough contour first via "fast" CS process and then add fine structures and complex features through "slow" SLM. The experimental results show that it is feasible to deposit SLM part onto CS part with good interfacial bonding. However, the CS parts must be subject to heat treatment to improve their cohesion strength before being sending for SLM processing. Otherwise, the high tensile residual stress generated during SLM process will cause fracture and cracks in the CS part. After heat treatment, pure copper deposited by CS undergoes grain growth and recrystallization, resulting in improved cohesive strength and release of the residual stress in the CS parts is released. The tensile test on the SLM/CS interfacial region indicates that the bonding strength increased by 38% from 45±7 MPa to 62±1 MPa after the CS part is subject to heat treatment, and the SLM/CS interfacial bonding strength is higher than the CS parts. This study demonstrates that the proposed hybrid AM process is feasible and promising for manufacturing free-standing SLM-CS components.

Keywords: cold spraying; selective laser melting; microstructure characteristics; hardness and interfacial bonding strength

1. Introduction

Selective Laser Melting (SLM) is an additive manufacturing (AM) process where high-power laser is applied to selectively melt metallic powders layer by layer and eventually build a near-net-shape component. It offers the ability to rapidly produce a component having complex geometry with fine details, allowing for the customization of products at an acceptable cost, giving no material waste through recycling unprocessed powder. It is hence well recognized as the technology of future industry. Many researches have been conducted to study the manufacturing parameters, microstructure, and performance of SLM. Some investigations indicate that with optimized laser parameters and scanning strategies, high-density pure copper and other metal parts with excellent mechanical properties can be produced by SLM [1-5]. Due to the high cooling rate and fast solidification during the manufacturing process, SLM 316L stainless steel typically has a fine grain structure, thus having higher yield strength, tensile strength and hardness as compared to forged and casted stainless steel [6]. With heat treatment, such fine grains of SLM 316L stainless steel grow into coarse grain, resulting in a significant decrease in strength and an increase in ductility [7,8]. However, since laser is required to locally melt powder over a very small area in a manner of point by point

 doi:10.20944/preprints202309.0776.v1

and then layer by layer, the deposition rate of SLM process is rather low, which results in long manufacturing time, especially when making large components. This significantly limits the application of SLM technology in a broader field. Also, the printing efficiency of SLM process is relatively low. The processing speed of SLM is highly dependent on many factors, including processing powder materials, machine brands and models, processing parameters, and the complexity of the object to be printed. Generally, a deposition rate between 0.4 kg/h and 5.0 kg/h can be achieved for SLM [9-11].

Cold Spray (CS) is an emerging solid particle deposition and AM technology [12-16]. Feedstock powders are accelerated by a supersonic gas passing through a de-Laval nozzle and subsequently impact onto a substrate to form a coating or bulk structure. CS feedstock can be deposited onto various substrates without experiencing melting; thereby, defects associated with other fusion-based AM processes can be avoided in CS. Due to the deformation-induced dynamic recrystallization, the grains of CS 316L stainless steel are refined during deposition. Most importantly, the material deposition rate of CS is much faster than that of SLM [16]. For CS, the deposition rate of materials such as Al and Cu can easily reach dozens of kilograms per hour [17], which is far higher than that in SLM process. However, due to the lack of manufacturing precision, CS products typically have a near net shape but with simple geometry and rough surface in their as-fabricated state [14].

As discussed above and also well addressed in literature, SLM and CS each have unique advantages and drawbacks. The fusion-based SLM process excels in the production of complex parts which requires high spatial resolution but not in a time efficient manner, while the solid-state CS process builds component rapidly but lacks manufacturing accuracy [16]. Considering these, in 2018, Yin et al. have proposed a 'hybrid additive manufacturing' concept that combines SLM and CS to take the benefits of each process to realize fast and high-precision fabrication [14]. As preliminary studies, they successfully cold-sprayed metal materials onto substrates made by SLM and studied the CS/SLM interfacial microstructures, which is not difficult to implement. However, CS materials onto SLM substrate may not be frequently encountered in practical engineering application. A more realistic manufacturing route for the "hybrid" is to fabricate a bulk deposit with a rough contour first via CS and then add fine structures and complex features through SLM. Therefore, in this paper, in order to prove the feasibility of the aforementioned hybrid SLM/CS concept, we selected Cu as exemplar material, and used CS to make bulk Cu substrates, and then add fine features on the CS substrates via SLM. Following fabrication, the microstructures at the SLM/CS interfaces of the hybrid parts and bonding strength at the interface were also investigated.

2. Material and methods

Fig. 1 shows the schematic of the hybrid AM process. CS processes were conducted on a commercial CS system (PCS-1000, Plasma Giken, Japan) to fabricate thick plates for the following SLM processing. During the manufacturing process, the CS nozzle trajectory followed the standard zigzag pattern. Nitrogen is used as a propulsion gas. The SLM process was conducted on a commercial SLM machine (EOS M290, Germany) under high-purity argon environment (Oxygen content below 1%). The Cu plates made from the previous CS processes were flattened via electrical discharge machining (EDM) and then used as the substrates for the SLM part fabrication. The substrates were preheated to 80 °C before spreading powders. Laser scans in a zigzag pattern with an angle of 67° applied between adjacent layers. Detailed CS and SLM processing parameters are provided in Table 1.

Preprints (www.preprints.org) | NOT PEER-REVIEWED | Posted: 12 September 2023 doi:10.20944/preprints202309.0776.v1

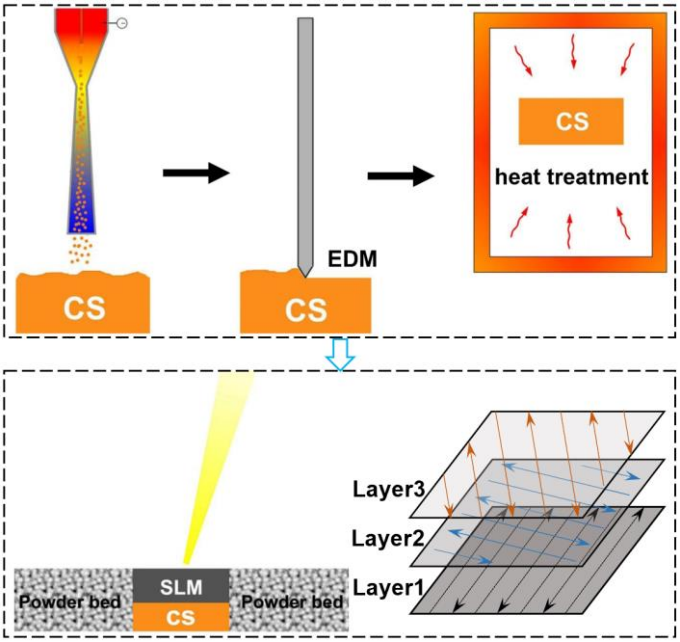

Figure 1. The flowchart of the hybrid AM process.

Table 1. Manufacturing parameters of the hybrid AM process.

CS	Gas	Pressure	Temperature	Standoff distance	Hatch distance	Nozzle moving speed
	N_2	**3.0 MPa**	**800 °C**	**35 mm**	**3.5 mm**	**50 mm/s**
SLM	Chamber	Laser spot diameter	Laser power	Layer thickness	Hatch distance	Laser moving speed
	Ar	100 μm	300 W	30 μm	80 μm	1.0 m/s

Spherical Cu powders (Beijing COMPO Advanced Technology, China) were used as raw materials for the fabrication of hybrid AM samples. The morphology of Cu powders is shown in Fig. 2. In addition, for studying how the heat treatment of the CS part influences the SLM/CS interfacial microstructure and bonding, a CS Cu substrate was subject to heat treatment at 500 °C for 4 h with a heating rate of 10 °C/min before SLM processing. Fig. 3a shows the photo of the Cu parts made by the hybrid AM process.

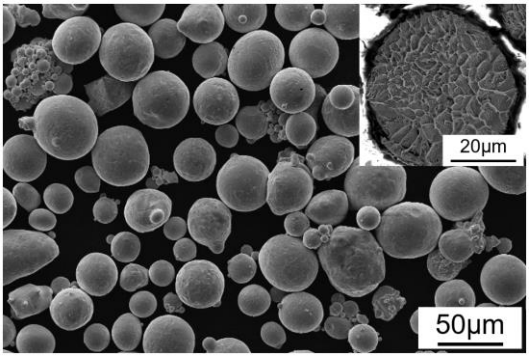

Figure 2. The morphology of the Cu powders used for SLM and CS.

Fig. 3a shows the as-fabricated part made with the hybrid AM process. Following fabrication, the microstructure of the hybrid AM parts was studied by OM (optical microscope, Leica, Germany) and SEM (Carl Zeiss ULTRA, Germany). All samples were polished using standard metallographic procedures with the final polishing step applied using 0.06 μm colloidal silica solution. The polished

Preprints (www.preprints.org) | NOT PEER-REVIEWED | Posted: 12 September 2023 doi:10.20944/preprints202309.0776.v1

Cu samples were etched with a regent of 5 g $FeCl_3$, 10 mL HCl and 100 mL water. The porosity of CS and SLM components was measured using binary image analysis with open-source image analysis software (ImageJ). The cross-sectional image was converted to binary format, and then porosity was calculated as the area ratio between the black pores and the white surface background. The porosity of each sample was considered as the average of three randomly selected micrographs in each sample cross-sectional. Struers DuraScan 70 was used to perform Vickers microhardness measurements in the cross-section using a load of 200 g (HV 0.2) and distance between indentations of 0.2 mm. In order to measure the interfacial bonding strength between the SLM and CS parts, non-standard dog-bone shaped tensile samples with a length of 10 mm, a gauge length of 4 mm, a width of 3 mm and a thickness of 3 mm was extracted from the SLM/CS interfacial region with the interface located exactly at the middle of the tensile samples as shown in the insert of Fig. 3b. The tensile samples were tested on Instron 5982 at a cross-head displacement rate of 0.2 mm/min.

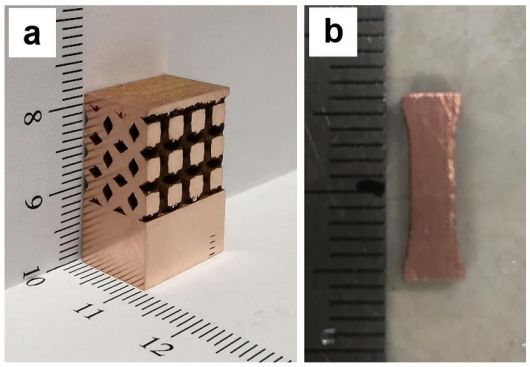

Figure 3. (a) The photo of the hybrid AM Cu part, and (b) non-standard dog-bone tensile sample.

3. Results and discussion

3.1. Microstructures of the hybrid AM sample (SLM Cu on as-fabricated CS Cu)

Fig. 4 shows the microscopic images of the interfacial microstructure of the SLM Cu deposited on as-fabricated CS Cu. As can be seen from the global view of the hybrid sample shown in Fig. 4a, a large crack was found beneath the SLM/CS interface in the CS part, which almost detached the SLM part from the CS part. However, interestingly, the SLM/CS interface seems clear and well bonded as shown in Fig. 4b and c. The reason for the crack is possibly the high tensile residual stress generated in the CS part that was caused by the high energy density of the laser during SLM process over the weak cohesion strength of the CS part [18]. It is well known that the strength of CS parts was normally much lower than the SLM counterparts since the interparticle bonding in CS parts is dominated by localized metallurgy and mechanical interlocking rather than complete metallurgy which dominates the interparticle bonding in SLM parts [19]. Such difference in microstructure can also be found in Fig. 4c in this study where interparticle boundaries that indicate incomplete metallurgical bonding between adjacent particles were clearly seen in the CS part after etching, while in the SLM part nearly all powder particles are fully melted to form complete metallurgy.

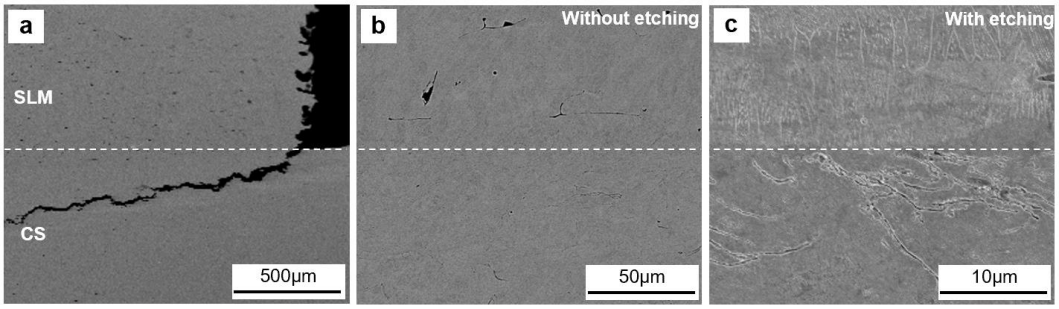

Preprints (www.preprints.org) | NOT PEER-REVIEWED | Posted: 12 September 2023 doi:10.20944/preprints202309.0776.v1

Figure 4. Interfacial microstructure of the hybrid SLM Cu on as-fabricated CS Cu observed by SEM. (a) global view of the SLM/CS part, (b) local SLM/CS interface, (c) etched local SLM/CS interface.

For further revealing the microstructural characteristics in the hybrid sample, Fig. 5 shows the etched microstructure of the SLM/CS part. Clearly, there was a significant difference in microstructure between the CS part and the SLM part. For the SLM part, the boundaries between adjacent tracks can be clearly seen, together with some micro-pores, as shown in Fig. 5a, which are typical microstructure for SLM Cu. Due to the thermal effect of the laser, metallurgical bonding occurs among Cu particles. For the CS part in the as-fabricated state, the interparticle boundaries could observed clearly after etching as shown in Fig. 5c. The particles in the CS part exhibit significant plastic deformation. The CS part seems to have lower porosity than the SLM part. The SLM/CS interface shown in Fig. 5b presents a large crack just beneath the interface. These findings are in consistent with the SEM observation shown in Fig. 4.

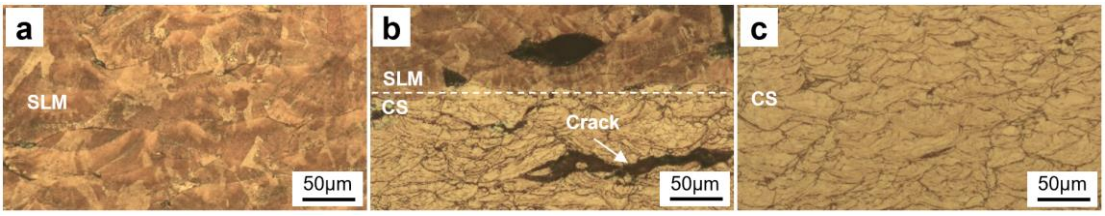

Figure 5. The cross-sectional microstructure of the hybrid SLM Cu on as-fabricated CS Cu after etching observed by OM. (a) SLM part, (b) SLM/CS interface, and (c) CS part.

During the hybrid AM process, the strength of the CS part is normally weak as discussed above, and the SLM process leads to the generation of tensile residual stress in the CS part. Therefore, once the tensile residual stress exceeds the strength of the CS Cu part, cracks nucleate and propagate at the location where residual stress reaches the maximum [20-22]. Such cracks will be significantly harmful to the bonding strength between SLM and CS parts. Although the formation of large crack in the CS part, the SLM/CS interface itself had no significant defects (e.g., large cracks and pores) as revealed by Fig. 4b and 4c. The SLM part well bond with the CS part. This phenomenon implies that it is feasible to deposit Cu on CS Cu via SLM as long as the formation of cracks is prevented. Our solution is hence to heat-treat the CS Cu part to improve its interparticle metallurgical bonding before it is subject to SLM processing, which will be described in the next section.

3.2. Microstructures of the hybrid AM sample (SLM Cu on heat-treated CS Cu)

Fig. 6 shows the interfacial microstructures of the hybrid AM sample (SLM Cu on heat-treated CS Cu). As can be seen, after the CS Cu substrate was heat treated, the CS part remained intact with no cracks found beneath the SLM/CS interface. This is because the interparticle bonding and overall cohesion strength of the CS part were significantly improved after heat treatment. This can be proved by the etched OM microstructure shown in Fig. 7 where interparticle boundaries could not be observed anymore in the CS Cu part. Instead, the CS part was characterized by large equiaxed grains and twining due to the recovery and recrystallization during the heat treatment [23,24]. Therefore, even though the SLM process caused high residual stress in the CS part, the high cohesion strength is able to withstand the nucleation of cracks. In addition, it is also seen from Fig. 6 and 7 that the SLM/CS interface exhibited good metallurgical bonding features and is free of significant metallurgical defects. These facts suggest that improving the CS Cu strength through conventional heat treatment can prevent the formation of cracks and provide a good SLM/CS interfacial bonding.

Preprints (www.preprints.org) | NOT PEER-REVIEWED | Posted: 12 September 2023 doi:10.20944/preprints202309.0776.v1

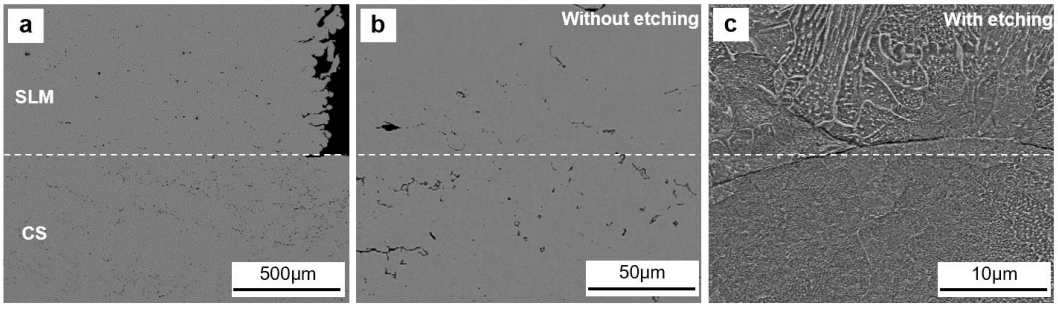

Figure 6. Interfacial microstructure of the hybrid SLM Cu on heat-treated CS Cu observed by SEM. (a) global view of the SLM/CS part, (b) local SLM/CS interface, (c) etched local SLM/CS interface.

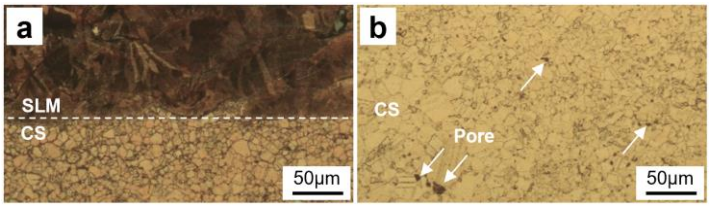

Figure 7. The cross-sectional microstructure of the hybrid SLM Cu on heat-treated CS Cu after etching observed by OM. (a) SLM/CS interface, (b) CS part.

3.3. Hardness and interfacial bonding strength of the hybrid AM Cu sample

Fig. 8 shows the hardness of the two hybrid samples measured across the SLM/CS interface. It is seen that heat treatment dramatically reduced the hardness of the CS part from 145 $HV_{0.2}$ to 40 $HV_{0.2}$ due to the grain growth. After heat treatment, the hardness difference between the SLM and CS parts were reduced [25].

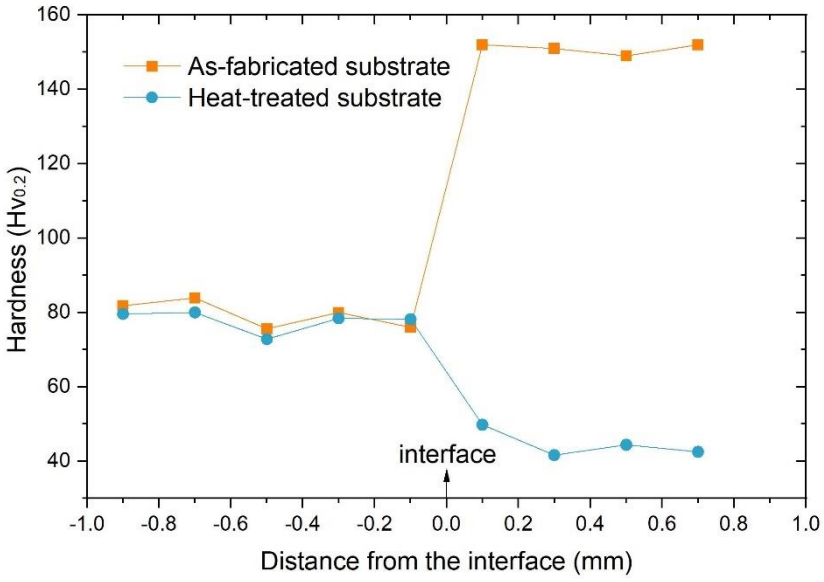

Figure 8. Hardness of the two hybrid samples measured across the SLM/CS interface.

Section 3.1 and 3.2 have confirmed that the interfacial bonding between the SLM and CS part could be improved by applying heat treatment to the CS part before SLM processing. In order to quantitively evaluate the interfacial bonding, Fig. 9 shows the stress-strain curves of the tensile samples extracted from the interfaces and the corresponding average strength. It is seen that the interfacial bonding strength was improved by 38% from 45±7 MPa to 62±1 MPa after the CS part was subject to heat treatment. The high interfacial bonding strength of heat-treated specimens is due to

Preprints (www.preprints.org) | NOT PEER-REVIEWED | Posted: 12 September 2023 doi:10.20944/preprints202309.0776.v1

the enhanced mass diffusion and recrystallization at the interface of CS and SLM components [26-28]. In addition, it is also found that both samples fractured in the CS part rather than the interface, which indicates that the SLM/CS interfacial bonding is stronger than the CS parts even though after heat treatment. For further studying the fracture mechanism, Fig. 10 shows the SEM images of the fracture surfaces of the tensile samples. The fracture mechanism of the as-fabricated CS part is in bi-mode with part of fracture through the interparticle boundaries (revealed by smooth particle surface and equiaxed grains) and the rest through the particles themselves (revealed by dimples). Similar fracture mechanism was also identified in the heat-treated CS part, but with new oxides on the particle surface caused by heat treatment and more dimples indicating better bonding.

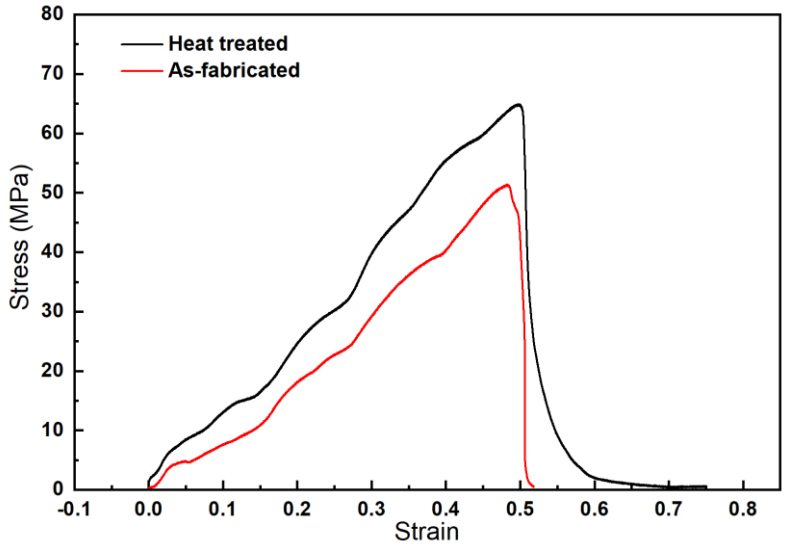

Figure 9. Stress-strain curves of the tensile samples extracted from the interfaces and the corresponding average strength.

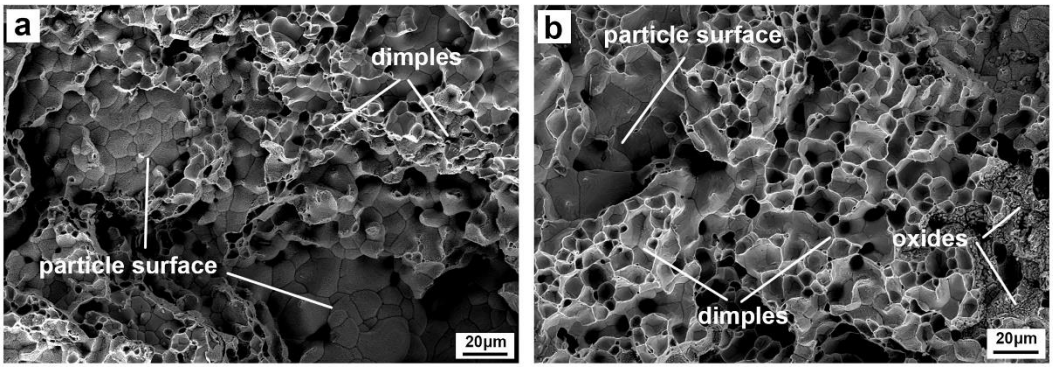

Figure 10. SEM images of the fracture surfaces of the tensile samples.

4. Conclusions

This paper presents a hybrid additive manufacturing (AM) process, combining fusion-based selective laser melting (SLM) and solid-state cold spraying (CS), for producing near-net-shape metal parts with high speed. The process begins with the deposition of a bulk deposit with a rough contour via the "fast" CS process, and then fine structures and complex features are added via the "slow" SLM process. It was found that SLM processing onto CS parts can lead to good interfacial bonding, but the CS parts must undergo heat treatment to improve the cohesion strength prior to SLM processing. Without addressing the high tensile residual stress caused by the SLM process, fractures and cracks may occur in the CS part. Results from the tensile tests on the SLM/CS interfaces indicated that the bonding strength increased by 38% from 45 ± 7 MPa to 62 ± 1 MPa following heat treatment.

This study provides evidence that the proposed hybrid AM process is feasible and promising for the rapid production of free-standing SLM-CS components.

Acknowledgement: This work was supported by Guangdong Academy of Sciences Special Fund for Comprehensive Industrial Technology Innovation Center Building (No. 2022GDASZH-2022010107); GDAS' project of Science and Technology Development (2022GDASZH-2022010203-003). We acknowledge the financial support.

References

1. S. Jadhav, S. Dadbakhsh, L. Goossens, J. Kruth, J. Humbeeck, K. Vanmeensel, Influence of selective laser melting process parameters on texture evolution in pure copper. Journal of Materials Processing Technology, 270 (2019) 47-58. doi:10.1016/j.jmatprotec.2019.02.022.
2. M. Colopi, L. Caprio, A. Demir, B. Previtali, Selective laser melting of pure Cu with a 1 kW single mode fiber laser. Procedia CIRP. 74 (2018) 59-63. doi:10.1016/j.procir.2018.08.030.
3. Z. Sun, X. Tan, S. Tor, W. Yeong, Selective laser melting of stainless steel 316L with low porosity and high build rates. Mater. Des. 126 (2017) 197-204. doi:10.1016/j.matdes.2016.05.035.
4. E. Liverani, S. Toschi, L. Ceschini, A. Fortunato, Effect of selective laser melting (SLM) process parameters on microstructure and mechanical properties of 316L austenitic stainless steel. J. Mater. Process. Technol. 249 (2017) 255-263. doi:10.1016/j.jmatprotec.2017.05.042.
5. G. Jia, H. Yang, H. Zhang, S. Xu, T. Peng, Y. Zhu, Electrical energy consumption and mechanical properties of selective-laser-melting-produced 316L stainless steel samples using various processing parameters. J. Clean. Prod. 208 (2018) 77-85. doi:10.1016/j.jclepro.2018.10.109.
6. Y. Wang, T. Voisin, J. McKeown, J. Ye, N. Calta, Z. Li, Z. Zeng, Y. Zhang, W. Chen, T. Roehling, R. Ott, M. Santala, P. Depond, M. Matthews, A. Hamza, T. Zhu, Additively manufactured hierarchical stainless steels with high strength and ductility. Nat. Mater. 17 (2018) 63–71. doi:10.1038/nmat5021.
7. K. Saeidi, X. Gao, F. Lofaj, L. Kvetková, Z. Shen, Transformation of austenite to duplex austenite-ferrite assembly in annealed stainless steel 316L consolidated by laser melting. Journal of Alloys & Compounds. 633 (2015) 463-469. doi:10.1016/j.jallcom.2015.01.249.
8. D. Kong, C. Dong, X. Ni, L. Zhang, J. Yao, C. Man, X. Cheng, K. Xiao, X. Li, Mechanical properties and corrosion behavior of selective laser melted 316L stainless steel after different heat treatment processes. Journal of Materials Science & Technology. 35 (2019) 1499-1507. doi:10.1016/j.jmst.2019.03.003.
9. D. Herzog, V. Seyda, E. Wycisk, C. Emmelmann, Additive manufacturing of metals. Acta Materialia. 117 (2016) 371-392. doi:10.1016/j.actamat.2016.07.019.
10. W. Yuan, R. Li, Z. Chen, J. Gu, Y. Tian, A comparative study on microstructure and properties of traditional laser cladding and high-speed laser cladding of Ni45 alloy coatings. Surface and Coatings Technology. 405 (2020) 126582. doi:10.1016/j.surfcoat.2020.126582.
11. W. Xi, B. Song, Y. Zhao, T. Yu, J. Wang, Geometry and dilution rate analysis and prediction of laser cladding. The International Journal of Advanced Manufacturing Technology. 103 (2019) 4695–4702. doi:10.1007/s00170-019-03932-7
12. W. Li, K. Yang, S. Yin, X. Yang, Y. Xu, R. Lupoi, Solid-state additive manufacturing and repairing by cold spraying: A review, J. Mater. Sci. Technol. 34 (2018) 440–457. doi:10.1016/j.jmst.2017.09.015.
13. Q. Wang, N. Ma, X. Luo, C. Li, Capturing cold-spray bonding features of pure Cu from in situ deformation behavior using a high-accuracy material model. Surface and Coatings Technology. 413 (2021) 127087. doi:10.1016/j.surfcoat.2021.127087.
14. S. Yin, X. Yan, C. Chen, R. Jenkins, M. Liu, R. Lupoi, Hybrid additive manufacturing of Al-Ti6Al4V functionally graded materials with selective laser melting and cold spraying, J. Mater. Process. Technol. 255 (2018) 650–655. doi:10.1016/j.jmatprotec.2018.01.015.
15. S. Yin, X. Yan, R. Jenkins, C. Chen, M. Kazasidis, M. Liu, M. Kuang, R. Lupoi, Hybrid additive manufacture of 316L stainless steel with cold spray and selective laser melting: Microstructure and mechanical properties, J. Mater. Process. Technol. 273 (2019). doi:10.1016/j.jmatprotec.2019.05.029.
16. S. Yin, P. Cavaliere, B. Aldwell, R. Jenkins, H. Liao, W. Li, R. Lupoi, Cold spray additive manufacturing and repair: Fundamentals and applications, Addit. Manuf. 21 (2018) 628–650. doi:10.1016/j.addma.2018.04.017.

17. O. Ozdemir, C. Widener, M. Carter, K. Johnson, Predicting the effects of powder feeding rates on particle impact conditions and cold spray deposited coatings. Journal of Thermal Spray Technology. 26(4) (2017) 1598-1615. doi:10.1007/s11666-017-0611-0.
18. A. Rttger, K. Geenen, M. Windmann, F. Binner, W. Theisen, Comparison of microstructure and mechanical properties of 316 L austenitic steel processed by selective laser melting with hot-isostatic pressed and cast material. Materials Science and Engineering: A. 678 (2016) 365-376. doi:10.1016/j.msea.2016.10.012.
19. S. Yin, J. Cizek, X. Yan, R. Lupoi, Annealing strategies for enhancing mechanical properties of additively manufactured 316L stainless steel deposited by cold spray, Surf. Coatings Technol. 370 (2019) 353–361. doi:10.1016/j.surfcoat.2019.04.012.
20. D. Xie, F. Lv, Y. Yang, L. Shen, Z. Tian, C. Shuai, B. Chen, J. Zhao, A Review on Distortion and Residual Stress in Additive Manufacturing, Chinese Journal of Mechanical Engineering: Additive Manufacturing Frontiers. 1 (3) (2022) 10039. doi:10.1016/j.msea.2019.01.037.
21. D.D. Gu, W. Meiners, K. Wissenbach, R. Poprawe, Laser additive manufacturing of metallic components: Materials, processes and mechanisms, Int. Mater. Rev. 57 (2012) 133–164. doi:10.1179/1743280411Y.0000000014.
22. I. Yadroitsev, I. Yadroitsava, Evaluation of residual stress in stainless steel 316L and Ti6Al4V samples produced by selective laser melting, Virtual Phys. Prototyp. 10 (2015) 67–76. doi:10.1080/17452759.2015.1026045.
23. X. Yan, C. Chang, D. Dong, S. Gao, W. Ma, M. Liu, H. Liao, S. Yin, Microstructure and mechanical properties of pure copper manufactured by selective laser melting. Materials Science and Engineering A. 789 (2020) 139615. doi:10.1016/j.msea.2020.139615.
24. J. Haubrich, J. Gussone, P. Barriobero-Vila, P. Kürnsteiner, E. Jägle, D. Raabe, N. Schell, G. Requena, The role of lattice defects, element partitioning and intrinsic heat effects on the microstructure in selective laser melted Ti-6Al-4V. Acta Mater. 167 (2019) 136-148. doi:10.1016/j.actamat.2019.01.039.
25. C. Körner, M. Ramsperger, C. Meid, D. Bürger, P. Wollgramm, M. Bartsch, G. Eggeler, Microstructure and Mechanical Properties of CMSX-4 Single Crystals Prepared by Additive Manufacturing. Metall Mater Trans A. 49 (2018) 3781–3792. doi:10.1007/s11661-018-4762-5.
26. Y. Li, X. Liang, Y. Yu, D. Wang, F. Lin, Review on Additive Manufacturing of Single-Crystal Nickel-based Superalloys. Chinese Journal of Mechanical Engineering: Additive Manufacturing Frontiers. 1 (2022) 100019. doi:10.1016/j.cjmeam.2022.100019.
27. S. Ci, J. Liang, J. Li, Y. Zhou, X. Sun, Microstructure and tensile properties of DD32 single crystal Ni-base superalloy repaired by laser metal forming. J Mater Sci Technol. 45 (2020) 23-34. doi:10.1016/j.jmst.2020.01.003.
28. S. Yin, N. Fan, C. Huang, Y. Xie, C. Zhang, R. Lupoi, W. Li, Towards high-strength cold spray additive manufactured metals: Methods, mechanisms, and properties. J Mater Sci Technol. 170 (2024) 47-64. doi:10.1016/j.jmst.2023.05.047.